Imprint lithography provides topographical nanocues to guide cell growth in primary cortical cell culture

Sijia Xie [a,*], Regina Luttge [a,b,*]

[a] MESA+ Institute for Nanotechnology, University of Twente, 7500AE Enschede, The Netherlands
[b] Department of Mechanical Engineering, Microsystems Group and ICMS Institute for Complex Molecular Systems, Eindhoven University of Technology, 5600MB Eindhoven, The Netherlands

ABSTRACT

In this paper, we describe a technology platform to study the effect of nanocues on the cell growth direction in primary cortical cell culture. Topographical cues to cells are provided using nanoscale features created by Jet and Flash Imprint Lithography, coated with polyethylenimine. We investigated nanoscaffolds with periodicities ranging from 200 nm to 2000 nm, and found that the samples with a period between 400 nm and 600 nm and a height of 118 nm showed highly ordered regions of neurites in a newly formed network with a preferential alignment tendency for astrocytes. Live/dead staining results showed that different materials, such as silicon, glass, and imprinted resist are rendered biocompatible by coating with polyethylenimine. This coating therefore allows for a free choice of scaffold materials and promotes good cell-substrate adhesion. From our results we conclude particular length scales of nanoscaffold can impose a degree of order on cell spreading behavior in a complex cellular brain-on-a-chip network, which could thus be used to emulate ordered brain regions and their function *in vitro*.

© 2014 Elsevier B.V. All rights reserved.

1. Introduction

In nature, ordered brain regions are formed during development [1]. Understanding this coordinated growth mechanism will become paramount in the design of brain-on-a-chip disease models of the brain. One of the most important factors for *in vitro* neuronal cell culturing on-chip is to provide a proper environment. The function of the neuronal cells is influenced by the so-called extracellular matrix (ECM) that provides a physical scaffold for the cells to adhere to as well as chemical cues for neuronal cell growth and morphological changes [2]. Researchers have made advances in studying the effect of surface topography on neuronal cells *in vitro* and seek to emulate the properties of the ECM with the help of micro- or nano-fabrication techniques. In these previous works the authors described that the confinement provided by micro scale patterns can induce neuronal cell attachment and direct neurite outgrowth [3–5]. In addition, nanostructures could be utilised as interconnecting spots to study neuronal cell adhesion [6,7]. These approaches provide us with various strategies to mimic the microenvironment of the ECM

and study its influence on brain function. However, the aforementioned studies mostly focus on the interaction between substrates and cells of certain cell lines.

In this work, we present an *in vitro* study of primary cells from the cortex (CTX) of new born rats on nanoscaffolds. For the present study, we chose to fabricate the nanoscaffolds by Jet and Flash Imprint Lithography (J-FIL™), a cost-effective, high-throughput nanopatterning method (for details of the various nanoimprint approaches, see, for example, the review by Guo [8]).

It is the ultimate goal of our research to design a device that applies nanomechanical actuation to modulate brain functions. We hypothesise that the nanoscaffolds with the dimensions investigated, here, which can lead to ordered neurite outgrowth may also influence signal transduction in the neurite network via the mechanism of mechanotransduction at the cellular adhesion points, if they can be dynamically adjusted [9]. However, we must first understand the interaction of neuronal cells with specific pattern geometries, and determine which may be suitable to align CTX into ordered networks similar to those found in the naturally developed brain. To realise such a brain-on-a-chip concept, we must also identify suitable cell culture conditions, as well as dimensions and fabrication processes parameters for the nanoscaffold. Ideally, we can determine, and replicate, those properties of the natural ECM which influence directional neuronal cell

* Corresponding authors at: MESA+ Institute for Nanotechnology, University of Twente, 7500AE Enschede, The Netherlands. Tel.: +31 068632183.
E-mail addresses: s.xie@utwente.nl (S. Xie), r.luttge@tue.nl (R. Luttge).

spreading. In this study, we investigated imprinted nanoscaffold periodicities ranging from 200 nm to 2000 nm. Cell culture results have yet to be obtained for the complete variety of dimensions, including specific ridge-groove ratios, that we have fabricated, but our results so far demonstrate that the culture of CTX on poly-ethlenimine (PEI)-coated nanoscaffolds with length scales between 400 nm and 600 nm show that the nanogrooved surface provides clear directional guidance to neuronal cells in comparison to a flat surface as a control. In this paper we describe the experimental method for generating the nanoscaffold technology platform and demonstrate its potential for advanced brain-on-a-chip studies using cell viability and immunostaining techniques. We also employ scanning electron microscopy (SEM) to investigate the interactions at the sub-cellular scale.

2. Materials and methods

2.1. Nanoscaffolds

Grooved nanoscaffolds were fabricated by Jet and Flash Imprint Lithography (J-FIL[TM]). Non-Silicon Monomat (Molecular Imprints Inc.) was used as a resist for J-FIL using an Imprio55 machine (Molecular Imprints, Inc.). A commercial quartz stamp (IMS Chips) fabricated by electron beam lithography and reactive ion etching was applied during J-FIL with a set of variations for the ridge-to-groove ratio (R/G) and pattern periods (P) previously designed

and manufactured [10]. Table 1 displays the dimensions of the structures in the stamp used in the experiment.

Fig. 2.1(1–4) shows the schematic outline of the J-FIL process. Before imprinting, a layer of 60 nm bottom anti-reflective coating (DUV30J; Brewer Science) was spin-coated on the wafer at 3000 rpm and baked at 120 °C for 120 s to improve the adhesion of the resist. Then, droplets of liquid imprint resist (Non-Silicon Monomat) were dispensed on the pre-coated wafer according to the optimised J-FIL process previously developed for this stamp [10]. From previous work the residual layer thickness is known to be 40 nm, while the imprinted resist height corresponds to approximately 100 nm, matching the height of the stamp. Both 100 mm dia. P-type ⟨100⟩ double-sided polished silicon (Si) (Okmetic) and 100 mm dia. borofloat glass (Schott) wafers were used as substrates for nanoscaffolds. When the stamp was pressed onto the substrate, the liquid resist droplets formed a continuous thin layer and filled the structures of the stamp because of capillary force (Fig. 2.1(2)). After leveling the contact force between the stamp and the substrate, the resist was poly-merised by UV exposure while the template was still in contact with the resist film (Fig. 2.1(3)). The stamp was detached once the resist was fully hardened (Fig. 2.1(4)). Each of the processed wafers was imprinted by step and repeat with a centered 2 × 2 array. Subsequently, the patterned region of the wafer level nano-scaffolds were cut into 9 × 9 mm pieces to fit a standard 24-well tissue culture plate.

Table 1
Dimension of nanostructures in the quartz stamp.

| No.	Ridge width (nm)	Groove width (nm)	Pattern period (nm)	No.	Ridge width (nm)	Groove width (nm)	Pattern period (nm)	No.	Ridge width (nm)	Groove width (nm)	Pattern period (nm)
1	770	230	1000	10	370	230	600	19	120	480	600
2	470	130	600	11	220	380	600	20	570	230	800
3	420	180	600	12	170	430	600	21	400	400	800
4	500	500	1000	13	150	150	300	22	200	200	400
5	100	100	200	14	120	180	300	23	120	280	400
6	180	130	300	15	270	130	400	24	1340	660	2000
7	220	780	1000	16	370	130	500	25	170	580	750
8	270	180	450	17	120	380	500	26	220	580	800
9	170	280	450	18	570	180	750	27	660	1340	2000
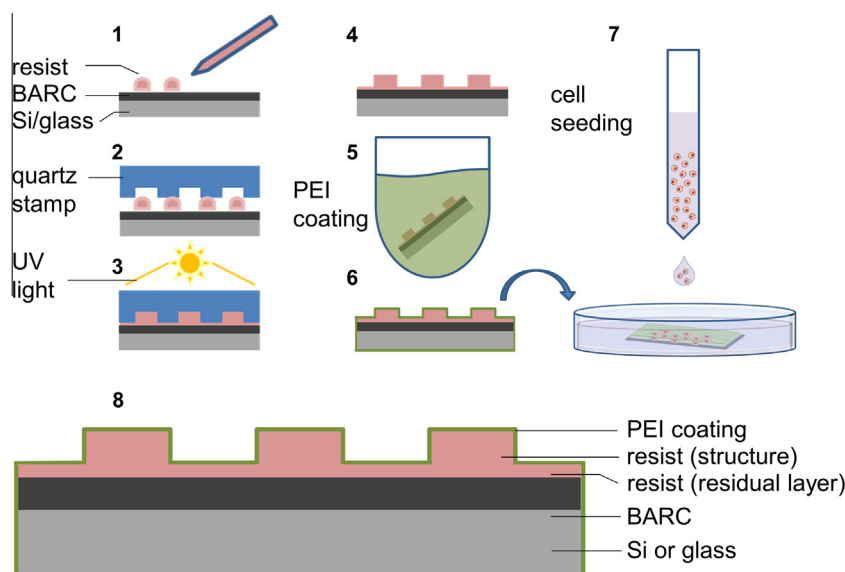
Fig. 2.1. Fabrication scheme and preparation of the nanoscaffold for cell culture. (1) Dispense the resist; (2) resist fills into the structures of the stamp through capillary force; (3) polymerise and harden the resist by UV exposure; (4) detach imprinted nanoscaffolds from stamp; (5) coat imprinted nanoscaffolds in PEI solution; (6) coated nanoscaffolds are ready to use; (7) seed CTX cell onto coated nanoscaffolds and start *in vitro* culturing; (8) profile of coated resist nanoscaffolds in detail.

All of these substrates above were treated in oxygen plasma for 1 min immediately before cell seeding, so as to sterilize them and improve cell-substrate adhesion [11].

In additional experiments, branched PEI (approx. M.N. 60,000, 50 wt% aq. solution, Acros Organics, CAS: 9002-98-6) was used as a coating layer to investigate its influence on cell-substrate adhesion. Fig. 2.1(5, 6) shows the PEI coating process of the imprinted resist nanoscaffolds, and the same process can be used for coating silicon or glass substrates for cell culturing. The PEI coating solution was prepared with a concentration of 50 µg/ml in sterile milliQ water. Substrates with resist or cleaned Si or glass nanoscaffolds were first treated with oxygen plasma and subsequently immersed in coating solution at 37 °C, for a minimum duration of 2.5 h or overnight. Before culturing, residual solution was removed by applying suction via a sterilized dropper and the substrates were air-dried in a biological safety cabinet. The coated nanoscaffolds were then ready for cell seeding (Fig. 2.1(7)). A detailed profile of the coated resist nanoscaffolds is displayed as an example in Fig. 2.1(8).

It is known that the abundant amino groups in the molecule of branched polyethylenimine (PEI) attract the negatively-charged cell membrane, effectively improving neuronal cell adhesion and spreading on substrates in a 2D culture [12]. These previous findings suggest that cell spreading and viability may be relatively independent of substrate material once a PEI coating has been applied. To determine the compatibility of our PEI-coated nanoscaffold material stack with CTX cells after cutting the pieces for the cell culture experiments (see Fig. 2.1, Section 2.3), we evaluated CTX cell viability first on control samples, consisting of untextured (flat) pieces of silicon and glass with and without PEI coating.

2.2. Geometrical characterisation of nanoscaffolds

Atomic force microscopy (AFM; Bruker ICON) was used to characterise the structure of the nanoscaffolds. AFM data were recorded and depicted as 3D models with Nanoscope 8.15 software (Bruker Corporation). Sectional profiles of the nanoscaffolds were drawn with origin7.5 (OriginLab).

2.3. Culturing CTX cells

CTX cells were isolated from new-born rat's brain and dissociated in R12H medium [13] with an approx. density of $3 * 10^6$ cell/ml, then seeded on the prepared substrates in a 24-well plate (Fig. 2.1(7)). Antibiotics were added in the medium at 0 day in vitro (DIV) to prevent infection. From 2 DIV, normal R12H was refreshed every 2 days until the in vitro culturing was terminated.

2.4. Fluorescent staining of CTX cells

A live/dead cell viability assay was performed after 8 DIV to evaluate the compatibility of the surface material of the nanoscaffolds to CTX cells, according to the standard procedure provided by Sigma Aldrich (04511 cell stain double staining kit).

To study the behavior of different types of neuronal cells in the primary CTX cell culture, we use Anti-MAP2 antibody (rabbit; Sigma Aldrich, M3696; 1:200), Anti-GFAP antibody (goat; Sigma, SAB2500462; 1:100), and Monoclonal Anti-CNPase antibody (mouse; Sigma Aldrich, C5922; 1:200) as the first antibodies in immunostaining, and Anti-Rabbit IgG (H+L), highly cross-adsorbed, CF™ 594 (Sigma Aldrich, SAB4600099; 1:200), Anti-Goat IgG (H+L), highly cross-adsorbed, CF™ 488A (Sigma Aldrich, SAB4600032; 1:200), and Anti-Mouse IgG (H+L), highly cross-adsorbed, CF™ 555 (Sigma Aldrich, SAB4600060; 1:200) as the second antibodies (all antibodies are produced in donkey), corresponding respectively to neuron, astrocyte and oligodendrocyte by specific binding.

The procedure for immunostaining referred to is the one provided by the Yale Center for High Throughput Cell Biology [14].

Optical fluorescence microscopy (Leica, DMI5000M) was used to observe and image the staining results. Images were analyzed with the Leica application suite software (Leica Microsystems, LAS05160).

2.5. Preparing cells for scanning electron microscopy

To prepare the cells for scanning electron microscopy (SEM; JEOL5610, JEOL USA, Inc.) and cross sectional SEM (Focused Ion Beam System, FIB; FEI Company™), cells were fixed and dehydrated as follows. First, the cells were prefixed for 30 min with 4% formaldehyde in 0.1 M phosphate buffered saline (PBS; Sigma Aldrich, D8537). After initial fixation, cells were gently rinsed with PBS 4 times. Then post-fixation and dehydration of cells was performed with 2:1 (v:v) ethanol (Assink Chemie) and hexamethyldisilazane (HMDS; BASF), 1:2 (v:v) ethanol and HMDS, 100% HDMS in sequence, each for 15 min. Finally, HMDS was removed and the cells were air-dried in a biological safety cabinet overnight.

The dehydrated samples were sputter-coated (Polaron,E5000 sputter coater) with a 10 nm thick Au/Pd (80%/20%) layer for SEM observation. To generate a cross sectional cut, focused ion beam with 30.0 kV and 0.92 nA was used for etching, and focused ion beam with 30.0 kV 0.28 nA for fine milling.

3. Results and discussion

3.1. Geometrical characterisation of nanoscaffolds

Fig. 3.1 depicts AFM images of three examples of the nanoscaffolds imprinted in resist. The ridges have average heights of 118 nm ($\sigma = 1.8$, $N = 4$) and widths of 128 nm ($\sigma = 1.9$, $N = 4$), 278 nm ($\sigma = 1.9$, $N = 4$) and 1329 nm ($\sigma = 0$, $N = 3$).

The examples in Fig. 3.1 revealed a smooth and flat top surface of the nanoridges, indicating good pattern fidelity in the pattern transfer from the stamp to the resist to be used repetitively in the biological experiments. Scaffolds with or without PEI coating showed no obvious differences by AFM, suggesting that the PEI forms a thin conformal layer around the nanoscaffold material stack.

3.2. Cell viability on different scaffold materials

Double fluorescent live/dead cell staining results indicate the viability of cells and therefore the compatibility of substrate materials with CTX cells. As shown in Fig. 3.2 after 8 DIV, CTX cells engaged a very low amount of surface area on the bare Si and glass surfaces. In contrast, cells cultured on surfaces with PEI coating showed a confluent cell coverage without overlap of cell clusters that would limit cell-survival [12]. Fig. 3.3 shows a graphical representation of the cell viability analysis performed for the substrates used in Fig. 3.2.

Culturing results on pristine surfaces of either silicon or glass (Fig. 3.2(a, c)) showed poor adhesion of cells onto these surfaces. Dying cells may lose adhesion and will therefore be washed off when the culture medium is refreshed [15], explaining the small number of red fluorescent spots that indicate dead cell nuclei. The PEI coating resulted in a significant improvement in cell-substrate adhesion, suggesting that it provides a promising environment for cell–cell interaction and especially for neuronal network formation. Furthermore, the use of a PEI coating appears to prevent any potential cytotoxicity of these materials to the cell culture, when they are used as a base wafer during nanoscaffold fabrication [16]. The chemical attraction to cells as well as the mitigation of
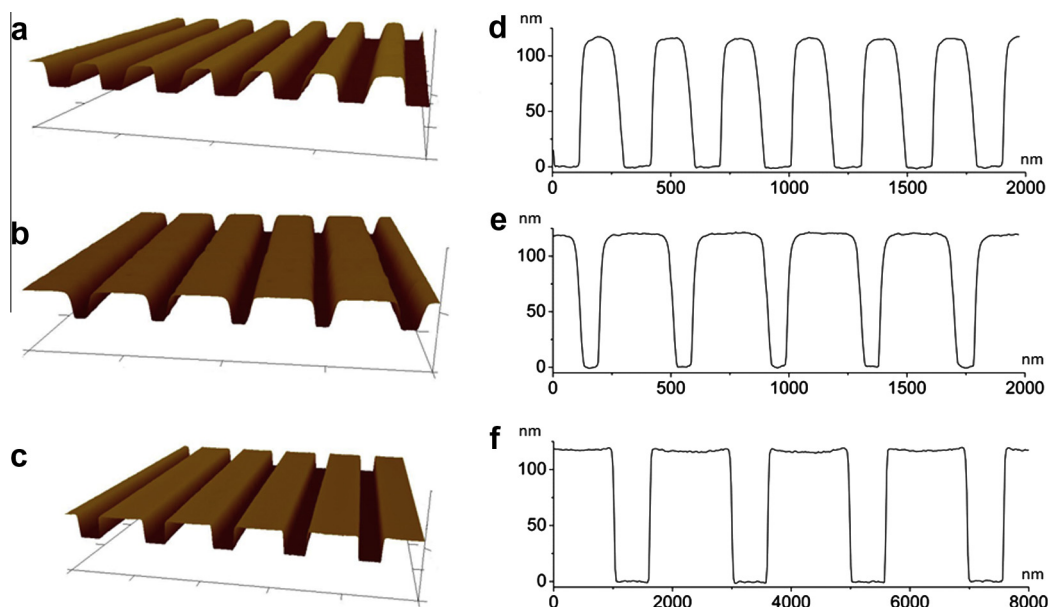
Fig. 3.1. Examples of three nanoscaffolds scanned by AFM. (a–c) depict 3D schematic diagrams of the nanoscaffolds, referring to the Nos. 6, 23, 27 in Table 1, respectively; (d–f) show the three cross-sectional profiles corresponding to (a–c).
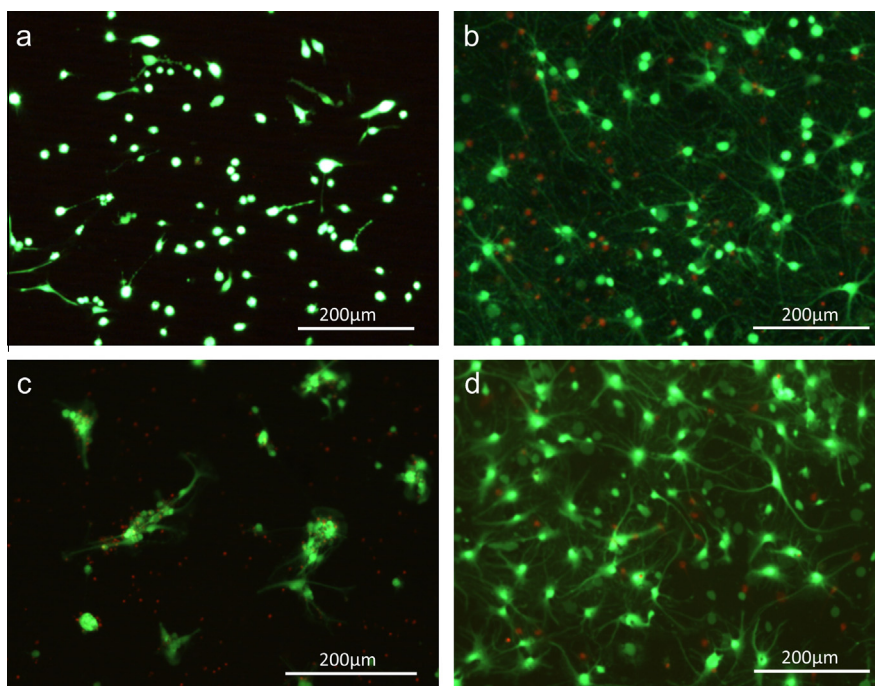

Fig. 3.2. Cell viability images on different materials after 8 DIV. The green label indicates living cells, while the red label indicates dead cells. (a) Flat silicon; (b) PEI coated flat Si; (c) flat glass; (d) PEI coated flat glass. (For interpretation of the references to colour in this figure legend, the reader is referred to the web version of this article.)

any material-related toxicity by the PEI coating relaxes the constraints on the types of materials which may be used and promotes reliable cell adhesion independent of the selected substrates (Fig. 3.2(b, d)).

3.3. Guided cell spreading on nanoscaffolds

Staining for cell viability on uncoated and coated resist nanoscaffolds confirmed the ability of the PEI coating to improve cell adhesion. The coating continues to function for the duration of the experiments (Fig. 3.4). For uncoated samples the number of cells were comparable to 0 DIV, however, clusters were widely observed on these pristine resist surfaces. The red fluorescent staining indicates a large number of dead cells inside the clusters (Fig. 3.4(b)), which could be a result of apoptosis due to an improper ECM, or lack of nutrients from the medium. Cells on the coated resist surface did not form such clusters (Fig. 3.4(c)), and displayed a similar degree of adhesion as previously shown in Fig. 3.2(b, d).

Although the degree of cell adhesion is not sufficient for forming neuronal network on a pristine resist surface, the outgrowth of the neuronal cell clusters already revealed a tendency for guiding. As shown in Fig. 3.4(a), bundles of neurites grew mostly in
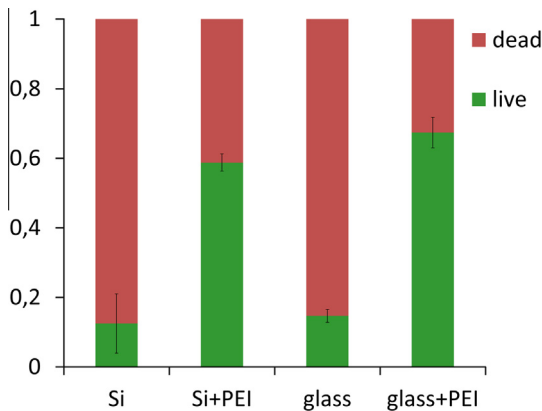
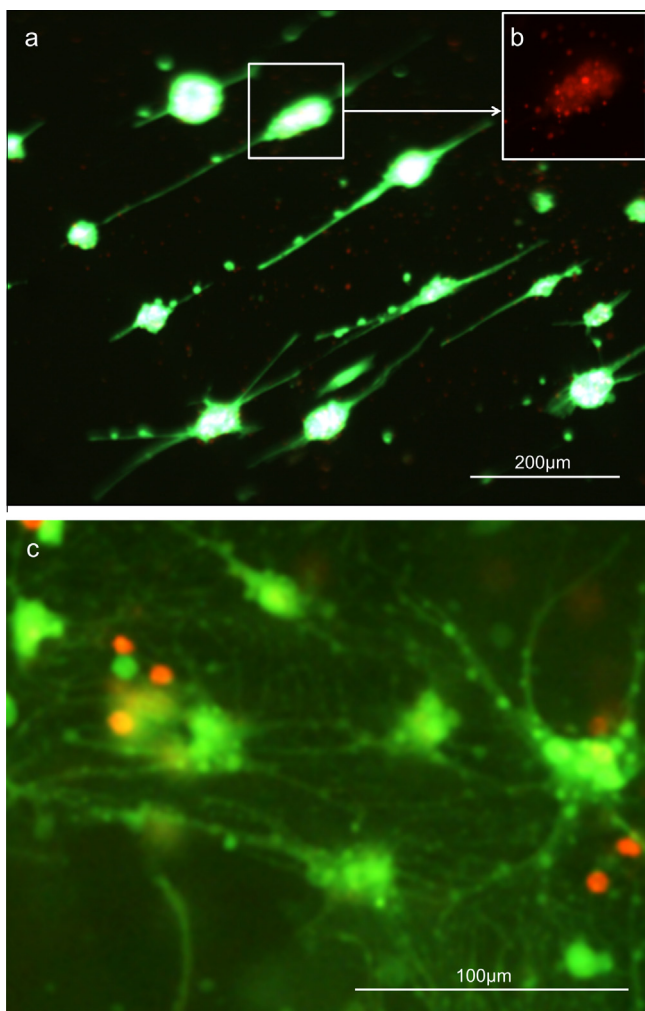**Fig. 3.3.** Cell viability on different materials after 8 DIV (number of sample N = 16).

Fig. 3.4. Cell viability on resist nanoscaffolds (No. 23, see Table 1) after 8 DIV. (a) Uncoated resist; (b) staining of dead cells inside of cluster; (c) PEI coated resist.

alignment with the nanogrooves. SEM images of the same culturing sample confirm that these neurites indeed demonstrate guided growth along the grooved nanoscaffolds (see Fig. 3.6(b)). The result depicted in Fig. 3.4(c) does not show such obvious guided cell spreading as shown in Fig. 3.6(a), because of the non-selectivity of the live/dead staining assay. This will be discussed in detail in the following paragraphs. Nevertheless, the confluent cell coverage and tendency to form a network without cluster formation after 8

DIV on the PEI coated nanoscaffolds confirms that our sample preparation method works effectively even after patterning and with the higher complexity of the material stack used in J-FIL.

While we observed the initial guiding effect already on a pristine nanoscaffold, immunostaining further revealed distinct behaviors for three types of CTX cells on PEI coated nanoscaffolds versus those exhibited on a flat control. As shown in Fig. 3.5(a), on a PEI-coated imprinted resist nanoscaffold, guided outgrowth occurs preferentially for astrocytes (green), while the same effect was not observed in neurons (red) and oligodendrocytes (orange). As a control, CTX cells grown on a PEI coated flat glass surface, showed random outgrowth of astrocytes, neurons and oligodendrocytes, respectively (Fig. 3.5(b)).

Among the dimensions presented in Table 1, we found the astrocytes of CTX cells had a relatively strong alignment with the pattern periods between 400 nm and 600 nm. Immunostaining results in Fig. 3.5(a) depict the significant aligning and guiding effect of the nanoscaffolds on astrocytes (recognised by the fluorescent labeled GFAP). This result indicates that the interconnection between the intermediate filament (IF) protein in the membrane of astrocytes and the nanoscaffolds might be comparable within the range of scales used in the experiment [17].

In addition, GFAP has been proposed as an important protein in the process of cell–cell adhesion, specially neuron-astrocytes interconnection [18]. Research based on neuronal cell lines has already revealed that neurons can align parallel with nanogrooved surfaces
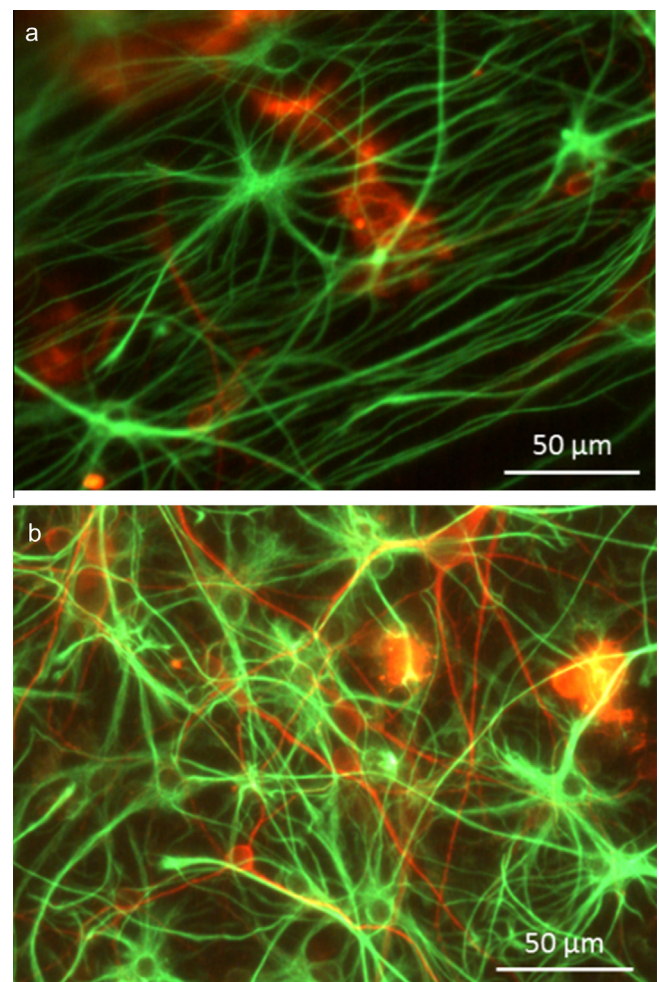

Fig. 3.5. Immunostaining of CTX cells on PEI coated samples after 12 DIV: (a) resist (nanoscaffold with 380 nm ridge width, 600 nm pattern period in reference to No. 11 in Table 1); and (b) flat glass substrate.

with groove width variations from 100 nm to 400 nm, and pattern periods from 200 nm to 1200 nm [3,19]. While in our study, when the primary cells were cultured collectively on the nanogrooved scaffolds, the guided alignment of neurons did not happen as distinctly as for the astrocytes. Considering the function of glial cells such as astrocytes and other supporting cells, the phenomenon could be explained as glial cells forming a supporting platform for neurons before the latter start to set up their network. This hypothesis could be further tested and verified by separating the primary cells and culturing each type singly and together. In addition, Lab-Chip integrated nanoscaffolds in conjunction with biomarker analysis may facilitate further *in vitro* brain research related to the formation of the ECM.

For a better understanding of the guidance mechanism for neurite outgrowth in this work, SEM images from both top-down and cross sectional views were processed to characterise the interaction at the cell–substrate interface at the sub-cellular scale. Fig. 3.6(a) shows the typical parallel alignment of single neurites observed on a PEI coated nanoscaffold. Fig. 3.6(b) visualises the connection between a neurite bundle and the nanogrooves after a cross-sectional cut. This result suggests that neurites interconnect preferably on top of the ridges.

In addition to the parallel alignment, seen in Fig. 3.6(a), tiny terminals that spread sideways from the neurites still showed random alignment. The interaction between the neuronal cells

and the nanoscaffolds needs to be studied in detail down to the molecular level. For example, previous work has demonstrated that the neurites interact with microgrooved pattern through actin [20]. However, questions concerning how the neurites connect with the nanoscaffold surface and how the former choose the orientation of their outgrowth still remain. More advanced studies will be needed to better understand the above results and the potential use of such nanoscale features in experiments for nano-mechanical neuromodulation. So far, the specific nanoimprint method, J-FIL, combined with PEI coating, investigated in this study allows us to robustly fabricate nanotopographical (physical) cues suitable for performing a systematic biological study on the effect of ordered cell growth during the network formation process for primary CTX. The results described here also close the gap to previous works on culture results with cell lines providing perspectives of the brain-on-a-chip concept.

4. Conclusion

We have developed nanoscaffolds with a systematic variation in length scale, which allow us to study the effect of ordering on neuronal brain functions. Nanoimprint lithography, specifically J-FIL, is shown to be a robust and reliable fabrication method that can be used to pattern a variety of substrate materials. Further, we have demonstrated the effects of the nanoscaffolds on rat primary CTX cells *in vitro*. Results show that patterns with periods between 400 nm and 600 nm guide the growth of neurites effectively. PEI coating ensures good cell-substrate adhesion and viability, thereby permitting a free choice of scaffold material. This broadens the number of potential fabrication techniques that may be used for future studies. Our experimental results demonstrate that astrocytes preferentially showed guided cell spreading. The biological relevance of this result for the coordination of neurophysiological activity across networks of neurons will be the subject of further investigations.
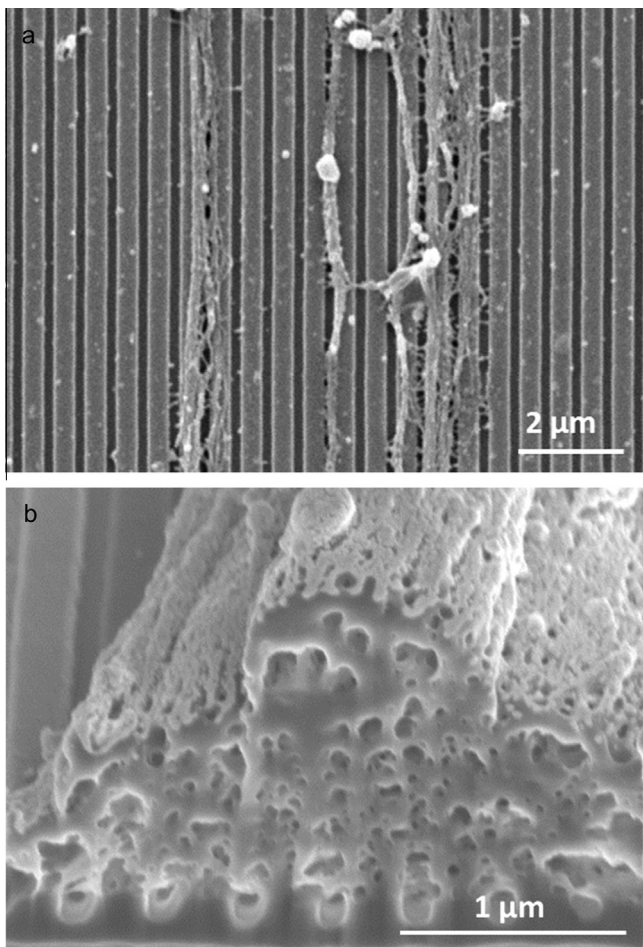
Fig. 3.6. SEM imaging of neurites and nanoscaffolds. (a) A couple of single neurites aligned along the nanogrooves (nanoscaffold with 380 nm ridge width, 600 nm pattern period in reference to No. 11 in Table 1); (b) cross section of a bundle of neurites grown along and atop of the nanogrooves (nanoscaffold with 280 nm ridge width, 400 nm pattern period in reference to No. 23 in Table 1).

References

[1] I. Bystron, C. Blakemore, P. Rakic, Nat. Rev. Neurosci. 9 (2008) 110–122, http://dx.doi.org/10.1038/nrn2252.
[2] L. Yu, N. Leipzig, M. Shoichet, Mater. Today 11 (2008) 36–43, http://dx.doi.org/10.1016/S1369-7021(08)70088-9.
[3] F. Johansson, P. Carlberg, N. Danielsen, L. Montelius, M. Kanje, Biomaterials 27 (2006) 1251–1258, http://dx.doi.org/10.1016/j.biomaterials.2005.07.047.
[4] N.S. Baek, J.H. Lee, Y.H. Kim, B.J. Lee, G.H. Kim, I.H. Kim, M.A. Chung, S.D. Jung, Langmuir (2011), http://dx.doi.org/10.1021/la103372v.
[5] E.A. Bremus-Koebberlinga, S. Beckemper, B. Koch, A. Gillner, J. Laser Appl. (2012), http://dx.doi.org/10.2351/1.4730804.
[6] L. Hanson, Z.C. Lin, C. Xie, Y. Cui, B. Cui, Nano Lett. 12 (2012) 5815–5820, http://dx.doi.org/10.1021/nl303163y.
[7] A.M.P. Turner, N. Dowell, S.W.P. Turner, L. Kam, M. Isaacson, J.N. Turner, H.G. Craighead, W. Shain, J. Biomed. Mater. Res. 51 (2000) 430–441, http://dx.doi.org/10.1002/1097-4636(20000905)51:3<430::AID-JBM18>3.0.CO;2-C.
[8] L.J. Guo, Adv. Mater. 19 (2007) 495–513, http://dx.doi.org/10.1002/adma.200600882.
[9] A. Curtis, C. Wilkinson, Biomaterials 18 (1997) 1573–1583, http://dx.doi.org/10.1016/S0142-9612(97)00144-0.
[10] R.V.d. Meer, PhD thesis (2013).

[11] T. Hoshino, I. Saito, R. Kometani, K. Samejima, S. Matsui, T. Suzuki, K. Mabuchi, Y.X. Kato, J. Biosci. Bioeng. 113 (2012) 395–398, http://dx.doi.org/10.1016/j.jbiosc.2011.11.003.

[12] R.W.F. Wiertz, PhD thesis (2010).

[13] H.J. Romijn, F. van Huizen, P.S. Wolters, Neurosci. Biobehav. Rev. 8 (1984) 301–334, http://dx.doi.org/10.1016/0149-7634(84)90055-1.

[14] http://www.sigmaaldrich.com/content/dam/sigma-aldrich/docs/Sigma/General_Information/1/yale-if-procedure.pdf.

[15] L.P. Wen, J. Biol. Chem. 272 (1997) 26056–26061, http://dx.doi.org/10.1074/jbc.272.41.26056.

[16] J. Choi, Q. Zhang, V. Reipa, N.S. Wang, M.E. Stratmeyer, V.M. Hitchins, P.L. Goering, J. Appl. Toxicol. 29 (2009) 52–60, http://dx.doi.org/10.1002/jat.1382.

[17] K. Kang, S.E. Choi, H.S. Jang, W.K. Cho, Y. Nam, I.S. Choi, J.S. Lee, Angew. Chem. Int. Ed. Engl. 51 (2012) 2855–2858, http://dx.doi.org/10.1002/anie.201106271.

[18] D.E. Weinstein, M.L. Shelanski, R.K.H. Liem, J. Cell Biol. 112 (1991) 1205–1213, http://dx.doi.org/10.1083/jcb.112.6.1205.

[19] A.M. Rajnicek, S. Britland, C.D. McCaig, J. Cell Sci. 110 (1997) 2905–2913.

[20] C. Oakley, D.M. Brunette, J. Cell Sci. 106 (1993) 343–354.